Title

Heart failure-induced brain myelin changes and differences between sexes.

Journal

Journal of Neuroscience Research, 101(10)

Authors

Roy, Bhaswati
Vacas, Susana
Ehlert, Luke
et al.

Publication Date

2023-10-01

DOI

10.1002/jnr.25229

Peer reviewed

HHS Public Access

Author manuscript

J Neurosci Res. Author manuscript; available in PMC 2024 October 01.

Published in final edited form as:

J Neurosci Res. 2023 October ; 101(10): 1662–1674. doi:10.1002/jnr.25229.

Heart Failure-Induced Brain Myelin Changes and Differences Between Sexes

Bhaswati Roy, PhD[a], **Susana Vacas, MD, PhD**[a], **Luke Ehlert, BA**[a], **Madeline Townsley, BS**[a], **Megan Carrier, MSHSA**[a], **Gregg C. Fonarow, MD**[b], **Mary A. Woo, RN, PhD**[c], **Rajesh Kumar, PhD**[a,d,e,f,*]

[a]Department of Anesthesiology and Perioperative Medicine, David Geffen School of Medicine, University of California Los Angeles, Los Angeles, CA

[b]Division of Cardiology, David Geffen School of Medicine, University of California Los Angeles, Los Angeles, CA

[c]School of Nursing, University of California Los Angeles, Los Angeles, CA

[d]Department of Radiological Sciences and Bioengineering, David Geffen School of Medicine, University of California Los Angeles, Los Angeles, CA

[e]Department of Bioengineering, University of California Los Angeles, Los Angeles, CA

[f]Brain Research Institute, University of California Los Angeles, Los Angeles, CA

Abstract

Heart failure (HF) leads to brain injury in autonomic, respiratory, mood, and cognitive control sites, revealed as tissue volume loss, altered metabolites, and impaired diffusion tissue properties. The extent of myelin changes in HF and variations within sexes are unclear. Our aim was to examine regional brain subcortical and white matter myelin integrity in HF patients over control subjects, as well as differences between sexes using T1- and T2-weighted clinical images. We acquired T1- and T2-weighted images from 63 HF patients and 129 controls using a 3.0-Tesla MRI scanner. Using T1- and T2-weighted images, ratio maps were computed, normalized to a common space, smoothed, and compared between groups (ANCOVA; covariates: age and sex; SPM12, false discovery rate, $p<0.01$), as well as between male vs female HF (ANCOVA; covariate: age; SPM12, uncorrected $p<0.005$). Multiple brain areas in HF showed decreased myelin integrity, including the amygdala, hippocampus, cingulate, insula, cerebellum, prefrontal cortices, and multiple white matter areas, compared to controls. Female HF patients showed more brain injuries in the parietal, prefrontal and frontal, hippocampus, amygdala, pons, cerebellar, insula, and corpus callosum compared to male HF patients. HF subjects showed compromised

[*]**Address for Correspondence:** Rajesh Kumar, PhD, Department of Anesthesiology, David Geffen School of Medicine at UCLA, 56-141 CHS, 10833 Le Conte Ave, University of California at Los Angeles, Los Angeles, CA 90095-1763, USA, Tel: 310-206-6133; 310-206-1679, Fax: 310-825-2236, rkumar@mednet.ucla.edu.

Author Contributions: All authors had full access to all the data in the study and take responsibility for the integrity of the data and the accuracy of the data analysis. Conceptualization, R.K.; Methodology, B.R. and R.K.; Investigation, B.R., S.V., L.E., M.T., G.F., M.W., and R.K.; Formal Analysis, B.R., L.E., M.T., M.C.; Writing- Original Draft, B.R., S.V.; Writing – Review & Editing, G.F., M.W., R.K., M.C.; Visualization, B.R.; Supervision, R.K.; Funding Acquisition, R.K.

Conflicts of interest: Bhaswati Roy, Susana Vacas, Luke Ehlert, Madeline Townsley, Megan Carrier, Gregg C. Fonarow, Mary A. Woo, and Rajesh Kumar declare that they have no conflict of interest.

subcortical and white matter myelin integrity, especially in sites regulating autonomic, respiratory, mood, and cognition, with more changes in females over males. These findings provide a structural basis for the enhanced symptoms identified in female over male HF patients with similar disease severity.

Keywords

Autonomic; Insula; Hippocampus; White matter; T1-weighted image; T2-weighted image

INTRODUCTION

Heart failure (HF) is a high-prevalence cardiovascular condition, and is the leading cause of hospitalization for adults in the United States. Further, HF-related changes are not localized to the cardiovascular system, but extend to the central nervous system with brain injury in autonomic, respiratory, mood, and cognitive control sites, as observed with various magnetic resonance imaging (MRI) techniques (Almeida et al., 2012; Kumar et al., 2011; Woo, Kumar, Macey, Fonarow, & Harper, 2009; Woo, Macey, Fonarow, Hamilton, & Harper, 2003; Woo et al., 2005; Woo et al., 2015). Widespread brain injury in HF subjects is accompanied with tissue volume and density loss (Almeida et al., 2012; Woo et al., 2003), altered metabolites (Woo et al., 2014), reduced cortical thickness (Kumar et al., 2015), and white matter changes (Kumar et al., 2011). However, the extent of whole-brain myelin changes in HF subjects is not clear. Myelin-insulating sheaths surrounding axons is crucial for the rapid and efficient transmission of electrical signals among neurons. Brain functions rely on the integrity of these layers, and diseases that lead to depletion of myelin often entail serious cognitive and physical impairments. An accurate assessment of myelin is vital for a comprehensive understanding of brain injury for this condition, as well as for the development of preventive strategies. Although various MRI methods, including T2-relaxometry, magnetization transfer imaging, diffusion tensor imaging (DTI)-based radial diffusivity, and diffusion kurtosis imaging-based radial kurtosis procedures can demonstrate the extent of myelin changes, these procedures have either poor spatial resolution or require long data acquisition times, as well as specialized image processing skills.

Brain myelin mapping, using the ratio of T1-weighted/T2-weighted images, was implemented to assess cortical myelin content. The ratio maps eliminate any image intensity bias related to the sensitivity profile of the radio frequency receiver coils and enhances the contrast-to-noise ratio for myelin content. The technique has been implemented in healthy controls (Grydeland, Walhovd, Tamnes, Westlye, & Fjell, 2013) and in other clinical condition, such as schizophrenia (Iwatani et al., 2015) to evaluate myelin content, and further validated with electrophysiological measures (Grydeland, Westlye, Walhovd, & Fjell, 2015). Thus, this ratio procedure can be applied for the assessment of myelin integrity in patients with HF.

HF prevalence is higher in males over females (~2:1; age range of 40–80 years of age), but the scenario is reversed after the age of 80 years. Since the life expectancy of female is ~5 years longer than that of male, long-term exposure to risk factors increases the prevalence

of HF in elderly female. Such sex differences might arise due to multiple factors associated with each sex group, including genetic and physiological basis, risk factors and etiology, pathophysiology, and variable treatment responses. Several genes on the Y chromosomes are associated with many cardiovascular risk factors, including increased blood pressure, low density lipoprotein cholesterol, and myocardial infarction. Other risk factors, such as acute coronary artery disease, diabetes, and valvular heart disease (aortic stenosis and mitral stenosis) lead to HF in a higher proportion of females over males. Although differences exist in disease prevalence among sexes, HF symptoms are worse in females over males with equivalent ejection fraction and ischemic burden. Previous studies indicate sex differences with regard to HF epidemiology, etiology, risk factors, pathogenesis, treatment responses, and prognosis (Rosengren & Hauptman, 2008; Shin, Hamad, Murthy, & Pina, 2012); however, there are no studies showing the variations in brain damage between male and female HF patients.

Our aim was to examine brain myelin integrity in HF patients using T1- and T2-weighted images compared to control subjects, as well as assess variations in brain changes between male and female HF patients. We hypothesized that myelin integrity is compromised in HF patients in various brain sites involved in autonomic, respiratory, cognitive, motor and neuro-psychologic regulation compared to control subjects, and that females with HF would exhibit more brain damage than males with HF.

MATERIALS AND METHODS

Subjects

Sixty three hemodynamically-optimized HF patients and 129 age- and sex-matched healthy control subjects were studied. Demographic, biophysical, and clinical variables of HF and control subjects are summarized in Table 1. HF subjects were diagnosed according to the American College of Cardiology diagnostic criteria (left ventricular ejection fraction <40%) (Jessup et al., 2009), and all subjects included in this study were with NYHA Functional Class I-III. HF patients were recruited from the Ahmanson-University of California at Los Angeles (UCLA) Cardiomyopathy Center and from the Los Angeles community. We performed brain MRI on HF subjects within one year of diagnosis to minimize variability in measures from disease onset. None of the HF patients had evidence or history of drug abuse, valvular congenital heart defects, pregnancy induced cardiomyopathy, stroke or carotid vascular disease, alcohol-induced cardiomyopathy or diastolic failure, smoking, or head injury. All HF patients underwent similar care and medications to achieve specific hemodynamic goals, including management with angiotensin receptor blockers or angiotensin-converting enzyme inhibitors, beta blockers, and diuretics; body weight and medication doses were stabilized for at-least six months before MRI examination. Control subjects were recruited from the UCLA Medical Center and Los Angeles area. All control subjects were healthy, without any medication and clinical history of cardiovascular disease, stroke, respiratory deficits, renal dysfunction, drug abuse, head injury, or neurologic and psychiatric disorders that may introduce brain changes. Subjects were excluded from the study if they were claustrophobic, carrying non-removable metal, pacemakers/implantable cardioverter-defibrillators, stents, or body weight more than 125 kg (scanner limitation).

All subjects gave written informed consent prior to participate in this study, and all study protocols were approved by the Institutional Review Board of the UCLA.

Sleep Quality and Daytime Sleepiness

All subjects were assessed for sleep quality and daytime sleepiness based on Pittsburgh sleep quality (PSQI) and Epworth sleepiness scale (ESS) (Carpenter & Andrykowski, 1998; Johns, 1992), respectively. These self-administered questionnaires were introduced on the same day of the MRI scan.

Assessment of depression and anxiety

Depression and anxiety symptoms of all HF patients and control subjects were evaluated using self-administered questionnaires, the Beck depression inventory (BDI-II) and the Beck anxiety inventory (BAI), respectively (Beck, Epstein, Brown, & Steer, 1988; Beck, Steer, Ball, & Ranieri, 1996). The questionnaires were administered on the same day of the MRI scan.

Cognition Assessment

The Montreal Cognitive Assessment (MoCA) was performed on all subjects for cognition assessment (Nasreddine et al., 2005). The test includes fast screening of various cognitive domains, including attention and concentration, executive functions, memory, language, visuo-constructional skills, conceptual thinking, calculations, and orientation.

Magnetic Resonance Imaging

Brain images were acquired from 3.0-Tesla MRI [Magnetom Tim-Trio (36 HF patients and 65 controls) and Prisma (27 HF patients and 64 controls); Siemens, Erlangen, Germany] scanners. Artifacts related to head-motion were minimized by placing foam pads on either side of the head during scanning. Two high resolution T1-weighted image volumes, covering the entire brain, were acquired with magnetization prepared rapid acquisition gradient-echo (MPRAGE) pulse sequence in the sagittal plane [repetition time (TR) = 2200 ms; echo time (TE) = 2.34 ms; inversion time = 900 ms; flip angle (FA) = 9°; matrix size = 256×256, 320×320; field of view (FOV) = 230×230 mm^2; slice thickness = 0.9, 0.72 mm). Whole brain proton-density and T2-weighted images were collected together using a dual-echo turbo spin-echo pulse sequence in the axial plane (TR = 10,000ms; TE1 = 12, 17ms; TE2 = 123, 134 ms; FA = 130°; matrix size = 256×256; FOV = 230×230 mm^2; slice thickness = 3.5, 4.0 mm). Two control subjects were scanned on both scanners (Tim-Trio and Prisma) for the purpose of validation to combine data from two different scanners.

On a subset of subjects (26 HF patients and 43 controls) DTI was performed in 3.0-Tesla MRI [Magnetom Prisma; Siemens, Erlangen, Germany] scanners using a single-shot echo planar imaging with twice-refocused spin-echo pulse sequence (TR = 12,200 ms; TE = 87 ms; FA = 90°; band-width = 1,345; matrix-size = 128×128; FOV = 230×230; slice thickness = 1.7, b = 0 and 800 s/mm^2, diffusion directions = 30). Two separate DTI series were collected with the same imaging parameters for subsequent averaging.

High-resolution T1-weighted, diffusion and non-diffusion weighted, PD-, and T2-weighted images of all HF and control subjects were visually evaluated for any gross brain pathology, such as tumors, cysts, or any other mass lesions, as well as motion artifacts. None of the subjects included in this study showed any serious brain pathology, head motion-related, or other imaging artifacts.

Calculation of Myelin Maps

Both high-resolution T1-weighted images were realigned to remove any potential variation between scans, averaged, and bias corrected. T2-weighted images were bias corrected as well. The bias corrected T1-weighted images were co-registered and re-sliced to the corresponding T2-weighted images. The ratio maps representing the myelin content from T1-weighted/T2-weighted images were computed using co-registered and bias-corrected T1- and T2-weighted images as follow:

$$\frac{T1-weighted}{T2-weighted}=\frac{\alpha_1 * x}{\alpha_2 * \frac{1}{x}}=\frac{\alpha_1}{\alpha_2}x^2=\beta x^2$$

where myelin integrity is represented by 'x'.α_1, α_2 are scaling factors related to bias field inhomogeneity of T1- and T2-weighted images, respectively.

Normalization and Smoothing of Myelin Maps

Myelin maps were normalized to Montreal Neurological Institute (MNI) common space using modified unified segmentation approach implemented in SPM12 software. The warping parameters for all directions were obtained from the corresponding bias corrected and re-sliced T1-weighted images via modified unified segmentation approach, and applied to the corresponding myelin maps. The normalized myelin maps were smoothed using an isotropic Gaussian filter (kernel size, 8 mm). We also normalized high-resolution T1-weighted images of control subjects to MNI space to derive whole-brain mean background images for structural identification.

Radial Diffusivity Calculation, Averaging, Normalization, and Smoothing

The diffusion tensor matrices were calculated using the Diffusion Toolkit software (Wang, Benner, Sorensen, & Wedeen, 2007). Using diffusion-weighted (b = 800 s/mm^2) and non-diffusion-weighted images (b = 0 s/mm^2), diffusion tensor matrices were calculated and diagonalized, and principal eigenvalues (λ_1, λ_2, and λ_3) were determined. The principal eigenvalues were used to calculate radial [$\lambda \perp = (\lambda_2 + \lambda_3)/2$] diffusivity (RD) values at each voxel, with voxel intensities on the maps showing the corresponding radial diffusivity values. The radial diffusivity maps and non-diffusion-weighted images, derived from each DTI series, were realigned and averaged. The realigned and averaged RD maps were normalized to MNI space using a unified segmentation approach and smoothed with a Gaussian filter (8mm).

Global Brain Mask

The averaged T1-weighted images of each subject were segmented into gray and white matter probability maps, and normalized to MNI space using SPM12. The normalized gray and white matter probability maps were averaged to create mean gray and white matter probability maps, respectively. The global brain mask was created by thresholding (gray and white matter > 0.3) and combining the global white and gray matter probability maps.

Region-of-Interest Analyses

Region-of-interest (ROI) analyses were performed to evaluate differences in mean ratio values in several brain sites between groups. Regional brain masks were created based on significant whole-brain voxel-by-voxel differences between groups for various brain regions, and values were extracted using these regional brain masks and corresponding smoothed myelin maps of HF and control subjects.

Validation for Combining Data

Two control subjects were scanned in the two different scanners (3.0-Tesla, Tim-Trio and 3.0-Tesla, Prisma) for validation of combining data from two scanners. Myelin maps of each subject were normalized and descalped to remove non-brain regions. Histograms of each normalized and descalped myelin maps were used to evaluate the differences in distribution of T1-weighted/T2-weighted values from two different scanners. Both histograms were identical, indicating no differences between scanners, and validating that data could be combined (Pike et al., 2018).

Comparison of Myelin Maps with RD Images

As an additional assessment, we compared the T1-weighted/T2-weighted maps with RD maps of the same controls and patients. DTI-based RD assesses water diffusion perpendicular to fibers and indicates myelin changes. Since we intended to compare different kinds of images that are characterized by different image intensities and contrasts, we evaluated the image intensity in a single ROI against the average intensity in the whole brain. We used the following formula:

$$t_{ROI} = \sqrt{n-1} * \frac{mean(\Delta_{ROI})}{sd(\Delta_{ROI})}$$

where $\Delta_{ROI} = [I_{ROI} - I_{Brain}]$ is the vector with the differences between ROI intensity and whole-brain mean intensity across subjects, and n is the number of subjects. The resulting t-score reflects differences of the ROI intensity from the mean calculated across the brain, taking between-subject variability into account. Determining t-scores for T1-weighted/T2-weighted and RD maps allowed us to assess their reliability across individuals, as well as consistency across different ROIs.

Statistical Analyses

The SPM12 and the IBM statistical package for the social sciences (IBM SPSS, v 27, Chicago, IL) software were employed for statistical analyses. Demographic, biophysical,

neuropsychologic, sleep, cognitive, and clinical characteristics between groups were assessed by independent samples t-tests ($p<0.05$) and Chi-square ($p<0.05$). To examine the consistency of histograms across scanners, the Kolmogorov test was performed to assess the differences in shape and the Wilcoxon rank-sum test was used to examine the differences in mean values.

We compared the smoothed myelin maps between 63 HF patients and 129 control subjects using analysis of covariance (ANCOVA), with age and sex included as covariates [SPM12; false discovery rate (FDR) $p<0.01$; minimum cluster-size 20 voxel]. In addition, smoothed myelin maps of 45 male HF patients were compared with 18 female HF patients using ANCOVA (SPM12; covariate: age; uncorrected $p<0.005$; 20 voxels). Brain regions with significant differences between groups were overlaid onto background images for structural identification.

We compared the smoothed myelin, as well RD maps between 26 HF patients and 43 control subjects using analysis of covariance (ANCOVA), with age and sex included as covariates (SPM12; uncorrected, $p<0.005$). Brain regions with significant differences between groups were overlaid onto background images for structural identification.

The mean ratio values between HF patients and control subjects, and male and female HF obtained from ROI analyses, were compared between groups using ANCOVA [IBM SPSS, Bonferroni corrected; HF vs Controls mean values: HF = 63, Control = 129, $F(1, 188)$, covariates: age and sex; Male vs Female HF mean values: male HF = 45, female HF = 18, $F(1, 60)$, covariate: age]. We considered a p-value less than 0.05 as statistically significant.

RESULTS

Demographics, Biophysical, Sleep, Neuropsychological, and Cognitive Variables

Demographic and other variables of HF patients and control subjects are summarized in Table 1. The type, stages, and etiology of HF along with medication and comorbid conditions are also detailed in Table 2. All HF patients had reduced left ventricular ejection fraction and were classified as the New York Heart association Functional Class I (13%), Class II (66%) and III (21%). No significant differences in age or sex emerged between HF patients and control subjects. However, BMI, blood pressure, sleep, mood, anxiety, and cognitive symptoms differed significantly between groups.

Biophysical, and other clinical variables of male and female HF patients are tabulated in Table 2. No significant differences were observed in age, BMI, heart rate, blood pressure, sleep, mood, and overall cognition between male and female HF patients, but males showed significant low performance in MoCA subscales of language and delayed recall compared to females.

Histograms Comparison

No significant differences were observed in histograms (Fig. 1) obtained from two different scanners in shape ($p = 0.56$, Wilcoxon rank-sum test) or consistency ($p = 0.46$, Kolmogorov test). Since no significant differences appeared between myelin maps from two different

scanners, subjects from both scanners [101 subjects (Magnetom, Tim-Trio) and 91 subjects (Magnetom, Prisma)] were combined.

Myelin Integrity Changes in HF over Control

Multiple brain areas showed altered myelin integrity across subcortical and white matter regions in HF patients when compared to control subjects. Subcortical sites with abnormal myelin values in HF patients emerged in the bilateral amygdala, cingulate, insula, basal forebrain, caudate, hippocampus, hypothalamus, putamen and thalamus. The widespread injury was observed in cerebellar and orbital and medial prefrontal cortices, extending to frontal, parietal, temporal, lingual, para-hippocampal and occipital area. Altered myelin integrity appeared in several white matter regions, including the cerebellar peduncles, corpus callosum, medulla, pons, dorsal raphe, and external capsule. Parietal, temporal, and occipital white matter regions also emerged with myelin changes in HF over control subjects [Fig. 2; HF = 63, control = 129, ANCOVA (covariates: age and sex), FDR corrected $p<0.01$]. Regional myelin values of HF and control subjects are summarized in Table 3 (Bonferroni corrected), where all brain sites show significant reductions in HF patients over control subjects. Regional myelin values from Tim-Trio (36 HF patients and 65 controls) and Prisma-Fit scanners (27 HF patients and 64 controls) are presented in Supplementary Tables 1 & 2 (Bonferroni corrected).

Myelin Changes in Male versus Female HF patients

Few crucial brain regions emerged with severe damage in female HF patients compared to male HF patients. These regions included the right parietal, ventral medial prefrontal and frontal cortices, hippocampus, amygdala, posterior cingulate, left pons, cerebellar peduncle, insula, temporal white matter, bilateral posterior corpus callosum, inferior and superior colliculus, temporal and occipital cortices, lingual gyrus, cerebellar cortices, para-hippocampal gyrus, and prefrontal cortices [Fig. 3; male HF = 45, female HF = 18, ANCOVA (covariate: age), uncorrected $p<0.005$]. Regional myelin values of male and female HF patients are summarized in Table 4 (Bonferroni corrected), with brain regions showing significant decrease in female over male HF patients. Glass-brain images of male HF compared to male control, and female HF compared to female control are presented in Supplementary Figure 1.

Myelin and RD maps

We compared the T1-weighted/T2-weighted maps with RD maps using the t-scores on 26 HF patients and 43 controls and found majority of brain regions had comparable t-scores with T1-weighted/T2-weighted and RD values (Table 5), indicating reproducibility and sensitivity of values obtained from T1-weighted/T2-weighted maps. The patient showed significant brain changes in comparable regions in T1-weighted/T2-weighted and RD analyses over control subjects [Fig. 4, HF = 26, control = 43, ANCOVA (covariates: age and sex), uncorrected $p<0.005$].

DISCUSSION

Regional brain myelin changes in HF subjects appeared in multiple subcortical areas, as well as white matter regions, sites that regulate autonomic, cognitive, and mood symptoms. The evaluation of myelin changes using T1-weighted/T2-weighted ratio has never been implemented before in HF patients, and the current procedure has the advantage of providing high-resolution images with shorter scanning times. Previous studies have shown several brain sites with myelin abnormality in HF, however, those sites were not as widespread as we observed here. The widespread myelin changes may result from hypoxia/ischemic processes, impaired cerebral autoregulation, and reduced cerebral blood flow (Roy et al., 2017), imposing a greater ischemic burden. In addition, O_2 desaturation from sleep disordered breathing commonly reported in HF patients may activate microglia, neuron apoptosis, and brain dysfunction that can affect wide-spread myelin integrity (Block & Hong, 2005). Our study shows that HF patients had significant changes in ESS and PSQI scores when compared to control subjects.

When comparing male HF patients with female HF patients, females showed greater myelin changes in crucial brain regions responsible for cognitive, emotional, and autonomic regulation. In addition, the widespread myelin injury in female HF patients might be due to differences in susceptibility to intermittent hypoxia (Li et al., 2014), and sex-based pathways of hypoxia/ischemia induced cell death, repair and plasticity (van de Looij, Chatagner, Huppi, Gruetter, & Sizonenko, 2011).

T1-weighted/T2-weighted Based Myelin Quantification

The original approach by Glasser et al (Glasser & Van Essen, 2011) showed myelin content across all cerebral cortex using MRI-derived T1-weighted/T2-weighted ratio maps. The increase in gray-white matter contrast on T1-weighted images and decrease in T2 relaxation values in both gray and white matter arise from myelin content (Koenig, 1991; Miot-Noirault, Barantin, Akoka, & Le Pape, 1997). The myelin content varies with both T1-weighted and T2-weighted intensity, but in opposite directions. Thus, the ratio maps explain the motivation to use this procedure. Moreover, the ratio method improves myelin localization by increasing the contrast to noise between heavily and lightly myelinated areas, mathematically canceling the MR-related intensity bias field related to the sensitivity profile of the radio frequency receiver coils, which are same for both types of images. In this study, we used T1-weighted/T2-weighted ratio maps to evaluate whole-brain myelin integrity in HF, as well as variability by sexes, which provided information for white as well as lightly myelinated gray matter regions (Glasser, Goyal, Preuss, Raichle, & Van Essen, 2014).

Myelin Integrity Changes in HF patients

The myelin changes in HF patients were observed in limbic-cortical-striatal-thalamic circuits, formed by connections between the orbital and medial prefrontal cortex, amygdala, hippocampal subiculum, ventromedial striatum, medial-dorsal and midline thalamic nuclei that regulate emotional behavior and are implicated in the pathophysiology of depression. Nearly 50% of HF patients report symptoms of depression, and the structural brain changes outlined in this study may contribute to these symptoms. Other HF symptoms include

restless legs, orthopnea, nocturia, and disturbances in sleep and changes in the sleep-wake pattern. The cognitive deficits observed in HF can be explicated by altered myelin integrity in the prefrontal cortex, which is involved in executive cognitive functions, such as planning and evaluating outcomes, in the frontal lobe, thought processing, in the parietal lobe, processing of sensory information into a perception, and in the temporal lobe, namely memory and naming. The neural circuit for cognition involving dorsal striatum and its cortical connections and corticoventral striatal loops, including the nucleus accumbens, amygdala, orbitofrontal cortex, anterior cingulate cortex, and the inferior-temporal cortex showed abnormal myelin integrity. The integrative control centers for autonomic functions, located in insular cortices, ventral medial prefrontal, cerebellar regions, and brainstem, show abnormal myelin integrity. Autonomic impulses arise in the brainstem and hypothalamus and receive higher control from the limbic sites, including the insular regions. The hypothalamus is a coordinating center for the motor control of numerous autonomic activity, including thermoregulation that is also impaired in HF patients.

Brain myelin changes in HF subjects were previously observed using DTI (Kumar et al., 2011). However, DTI processing has several limitations, including requirement of specialized data processing skills, as opposed to T1weighted/T2 weighted imaging processing. The usage of signal and tissue contrast information in obtaining myelin maps with high resolution T1-weighted images that resolve laminar differences show widespread myelin damage in our study, but also include the regions previously reported in this condition. Reduced myelin, indicating a thinner myelin sheath that allows water to penetrate faster, might have resulted from a range of pathological processes, including hypoxic/ischemic episodes. Oligodendrocytes, axon-supporting cells that contribute to myelin formation are susceptible to hypoxia and high CO_2, and can contribute to myelin depletion. Several other factors that can contribute to exaggerated myelin changes include the coexistence of sleep breathing disorders and diabetes, which independently induces brain injury.

Myelin Changes in Male HF patients over Female HF patients

Myelin changes were more widespread in female HF patients as compared to males. The differences might arise due to inherent biological alterations due to sex-related differences in the manifestation of the disease, treatment response, and the natural history of the disease. Different clinical guidelines leading to differences in care for male and female might also be a contributing factor. The pathophysiological mechanisms of HF, such as renin-angiotensin and sympathetic nervous system and sexual hormones (androgens, estrogens) affect cardiac function differently between sexes. The treatment of HF with beta-blockers and ACE inhibitors affects each sex differently, as is the case with Cytochrome P450 isoenzyme activity (Razzolini & Lin, 2015), leading to higher effectiveness of these drugs in male patients while potentially causing greater neuronal injury in females.

Although biophysical, sleep, and mood scores were not significantly different in male HF patients over female HF patients, cognition components, such as language and delayed recall, were significantly lower in males. Brain injury emerging in critical sites for cognition (hippocampus, parahippocampal gyrus, prefrontal and frontal cortices, posterior cingulate,

and lingual gyrus), mood (amygdala, insula, ventral medial prefrontal cortices, and posterior cingulate) and autonomic regulation (cerebellar cortices, inferior and superior colliculus, cerebellar peduncle, and corpus callosum) in female HF patients over male HF patients suggests a delay in the functional onset of deficits for female subjects.

Limitations

Heart failure patients enrolled in our study had multiple comorbidities, including depression and anxiety. Several brain areas, including anterior insula, anterior cingulate, and right ventral medial prefrontal cortex are involved in autonomic regulation, and same sites have overlapping functional regulation for depression and anxiety. Since autonomic sites are compromised in HF and those regions are involved in mediating mood functions as well, we believe that HF patients are showing such functional dysfunctions. Also, other factors including medication use, timing of the scan after heart failure, persistent blood pressure elevation might also contribute to brain changes. However, such elements have not been included in the statistical model due to unavailability of these parameters, and can be considered as limitations.

CONCLUSIONS

In this study, HF patients exhibited compromised myelin status in subcortical gray and white matter regions regulating autonomic, respiratory, cognitive, motor, and neuropsychologic functions. A range of pathological processes, including low cardiac output leading to ischemia, breathing symptoms causing hypoxia, endothelial dysfunction contributing to impaired cerebral autoregulation and reduced cerebral blood flow may contribute to such injury. Widespread myelin changes appeared more frequently in female HF patients over male HF patients with similar ejection fraction, indicating the basis for critical symptoms observed in females and suggesting the potential need for sex-based therapeutic strategies for reversal of these damages.

Supplementary Material

Refer to Web version on PubMed Central for supplementary material.

ACKNOWLEDGEMENTS

We thank Mrs. Karan Harada and Ms. Cristina Cabrera-Mino for their help with data collection.

Grant support:

This research work was supported by National Institutes of Health R01 NR-014669 and American Heart Association 17POST33440099 (BR). Dr. Vacas was supported by K23GM132795.

Data Availability Statement:

The data that support the findings of this study are available on request from the corresponding author. The data are not publicly available due to privacy or ethical restrictions.

References

Almeida OP, Garrido GJ, Beer C, Lautenschlager NT, Arnolda L, & Flicker L. (2012). Cognitive and brain changes associated with ischaemic heart disease and heart failure. Eur Heart J, 33(14), 1769–1776. doi:10.1093/eurheartj/ehr467 [PubMed: 22296945]

Beck AT, Epstein N, Brown G, & Steer RA (1988). An inventory for measuring clinical anxiety: psychometric properties. J Consult Clin Psychol, 56(6), 893–897. [PubMed: 3204199]

Beck AT, Steer RA, Ball R, & Ranieri W. (1996). Comparison of Beck Depression Inventories -IA and -II in psychiatric outpatients. J Pers Assess, 67(3), 588–597. doi:10.1207/s15327752jpa6703_13 [PubMed: 8991972]

Block ML, & Hong JS (2005). Microglia and inflammation-mediated neurodegeneration: multiple triggers with a common mechanism. Prog Neurobiol, 76(2), 77–98. doi:10.1016/j.pneurobio.2005.06.004 [PubMed: 16081203]

Carpenter JS, & Andrykowski MA (1998). Psychometric evaluation of the Pittsburgh Sleep Quality Index. J Psychosom Res, 45(1), 5–13. [PubMed: 9720850]

Glasser MF, Goyal MS, Preuss TM, Raichle ME, & Van Essen DC (2014). Trends and properties of human cerebral cortex: correlations with cortical myelin content. Neuroimage, 93 Pt 2, 165–175. doi:10.1016/j.neuroimage.2013.03.060 [PubMed: 23567887]

Glasser MF, & Van Essen DC (2011). Mapping human cortical areas in vivo based on myelin content as revealed by T1- and T2-weighted MRI. J Neurosci, 31(32), 11597–11616. doi:10.1523/JNEUROSCI.2180-11.2011 [PubMed: 21832190]

Grydeland H, Walhovd KB, Tamnes CK, Westlye LT, & Fjell AM (2013). Intracortical myelin links with performance variability across the human lifespan: results from T1- and T2-weighted MRI myelin mapping and diffusion tensor imaging. J Neurosci, 33(47), 18618–18630. doi:10.1523/JNEUROSCI.2811-13.2013 [PubMed: 24259583]

Grydeland H, Westlye LT, Walhovd KB, & Fjell AM (2015). Intracortical Posterior Cingulate Myelin Content Relates to Error Processing: Results from T1- and T2-Weighted MRI Myelin Mapping and Electrophysiology in Healthy Adults. Cereb Cortex. doi:10.1093/cercor/bhv065

Iwatani J, Ishida T, Donishi T, Ukai S, Shinosaki K, Terada M, & Kaneoke Y. (2015). Use of T1-weighted/T2-weighted magnetic resonance ratio images to elucidate changes in the schizophrenic brain. Brain Behav, 5(10), e00399. doi:10.1002/brb3.399 [PubMed: 26516617]

Jessup M, Abraham WT, Casey DE, Feldman AM, Francis GS, Ganiats TG, . . . Yancy CW (2009). 2009 focused update: ACCF/AHA Guidelines for the Diagnosis and Management of Heart Failure in Adults: a report of the American College of Cardiology Foundation/American Heart Association Task Force on Practice Guidelines: developed in collaboration with the International Society for Heart and Lung Transplantation. Circulation, 119(14), 1977–2016. doi:10.1161/CIRCULATIONAHA.109.192064 [PubMed: 19324967]

Johns MW (1992). Reliability and factor analysis of the Epworth Sleepiness Scale. Sleep, 15(4), 376–381. [PubMed: 1519015]

Koenig SH (1991). Cholesterol of myelin is the determinant of gray-white contrast in MRI of brain. Magn Reson Med, 20(2), 285–291. [PubMed: 1775053]

Kumar R, Woo MA, Macey PM, Fonarow GC, Hamilton MA, & Harper RM (2011). Brain axonal and myelin evaluation in heart failure. J Neurol Sci, 307(1–2), 106–113. doi:S0022–510X(11)00231–0 [pii] 10.1016/j.jns.2011.04.028 [PubMed: 21612797]

Kumar R, Yadav SK, Palomares JA, Park B, Joshi SH, Ogren JA, . . . Woo MA (2015). Reduced regional brain cortical thickness in patients with heart failure. PLoS One, 10(5), e0126595. doi:10.1371/journal.pone.0126595

Li QY, Feng Y, Lin YN, Li M, Guo Q, Gu SY, . . . Wan HY (2014). Gender difference in protein expression of vascular wall in mice exposed to chronic intermittent hypoxia: a preliminary study. Genet Mol Res, 13(4), 8489–8501. doi:10.4238/2014.October.20.25 [PubMed: 25366743]

Miot-Noirault E, Barantin L, Akoka S, & Le Pape A. (1997). T2 relaxation time as a marker of brain myelination: experimental MR study in two neonatal animal models. J Neurosci Methods, 72(1), 5–14. [PubMed: 9128162]

Nasreddine ZS, Phillips NA, Bedirian V, Charbonneau S, Whitehead V, Collin I, . . . Chertkow H. (2005). The Montreal Cognitive Assessment, MoCA: a brief screening tool for mild cognitive impairment. J Am Geriatr Soc, 53(4), 695–699. doi:10.1111/j.1532-5415.2005.53221.x [PubMed: 15817019]

Pike NA, Roy B, Gupta R, Singh S, Woo MA, Halnon NJ, . . . Kumar R. (2018). Brain abnormalities in cognition, anxiety, and depression regulatory regions in adolescents with single ventricle heart disease. Journal of neuroscience research, 96(6), 1104–1118. doi:10.1002/jnr.24215 [PubMed: 29315714]

Razzolini R, & Lin CD (2015). Gender differences in heart failure. Ital J Gender-Specifi c Med, 1, 15–20.

Rosengren A, & Hauptman P. (2008). Women, men and heart failure: a review. Heart Fail Monit, 6(1), 34–40. [PubMed: 18607520]

Roy B, Woo MA, Wang DJJ, Fonarow GC, Harper RM, & Kumar R. (2017). Reduced regional cerebral blood flow in patients with heart failure. Eur J Heart Fail, 19(10), 1294–1302. doi:10.1002/ejhf.874 [PubMed: 28560737]

Shin JJ, Hamad E, Murthy S, & Pina IL (2012). Heart failure in women. Clin Cardiol, 35(3), 172–177. doi:10.1002/clc.21973 [PubMed: 22389122]

van de Looij Y, Chatagner A, Huppi PS, Gruetter R, & Sizonenko SV (2011). Longitudinal MR assessment of hypoxic ischemic injury in the immature rat brain. Magn Reson Med, 65(2), 305–312. doi:10.1002/mrm.22617 [PubMed: 20859997]

Wang R, Benner T, Sorensen AG, & Wedeen VJ (2007). Diffusion Toolkit: A Software Package for Diffusion Imaging Data Processing and Tractography. Paper presented at the Proc. Intl. Soc. Mag. Reson. Med.

Woo MA, Kumar R, Macey PM, Fonarow GC, & Harper RM (2009). Brain injury in autonomic, emotional, and cognitive regulatory areas in patients with heart failure. J Card Fail, 15(3), 214–223. doi:10.1016/j.cardfail.2008.10.020 [PubMed: 19327623]

Woo MA, Macey PM, Fonarow GC, Hamilton MA, & Harper RM (2003). Regional brain gray matter loss in heart failure. J Appl Physiol (1985), 95(2), 677–684. doi:10.1152/japplphysiol.00101.2003 [PubMed: 12716866]

Woo MA, Macey PM, Keens PT, Kumar R, Fonarow GC, Hamilton MA, & Harper RM (2005). Functional abnormalities in brain areas that mediate autonomic nervous system control in advanced heart failure. J Card Fail, 11(6), 437–446. doi:10.1016/j.cardfail.2005.02.003 [PubMed: 16105635]

Woo MA, Palomares JA, Macey PM, Fonarow GC, Harper RM, & Kumar R. (2015). Global and regional brain mean diffusivity changes in patients with heart failure. Journal of neuroscience research, 93(4), 678–685. doi:10.1002/jnr.23525 [PubMed: 25502071]

Woo MA, Yadav SK, Macey PM, Fonarow GC, Harper RM, & Kumar R. (2014). Brain metabolites in autonomic regulatory insular sites in heart failure. J Neurol Sci, 346(1–2), 271–275. doi:10.1016/j.jns.2014.09.006 [PubMed: 25248953]

Significance

Brain injury in HF has been shown in multiple sites, however the impact and extent of myelin changes and variations within sexes is still unclear. Our study shows that HF patients exhibit compromised myelin status in subcortical gray and white matter regions that regulate autonomic, respiratory, cognitive, motor, and neuropsychological functions. Widespread myelin changes appeared more frequently in female over male HF patients with similar ventricular ejection fraction. These findings indicate that there is a structural basis for the critical symptoms observed in female patients, suggesting the potential need for sex-based therapeutic strategies for reversal of these damages.

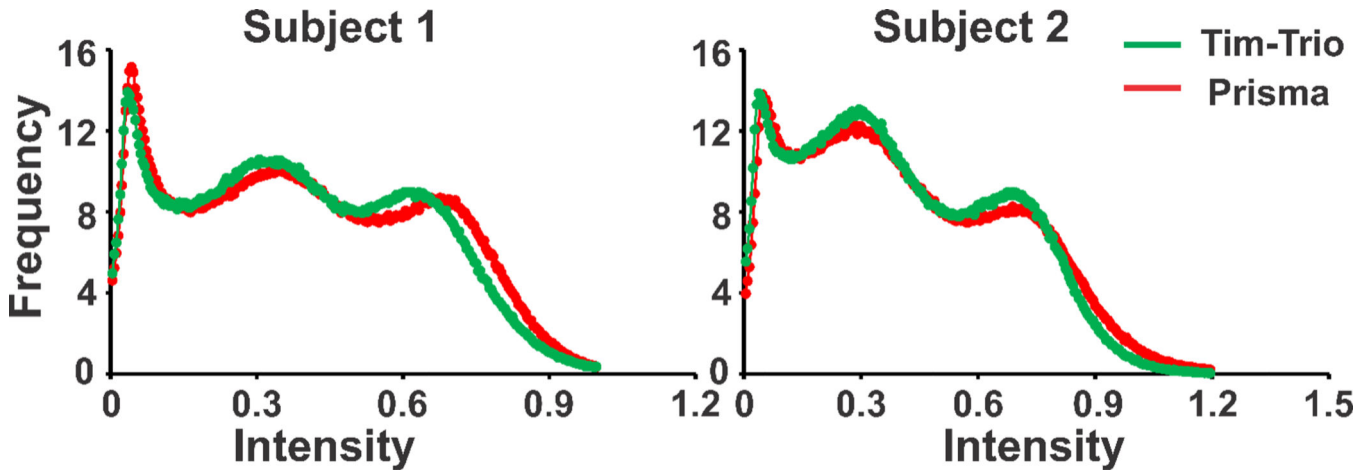

Figure 1:

T1-weighted/T2-weighted ratio histograms from two control subjects scanned on two different scanner platforms (3.0-Tesla, Magnetom, Prisma-Fit, and Tim-Trio). T1-weighted/T2-weighted ratio histograms were plotted for descalped T1-weighted/T2-weighted ratio maps obtained from Prisma-Fit (red) and Tim-Trio (green) scanners.

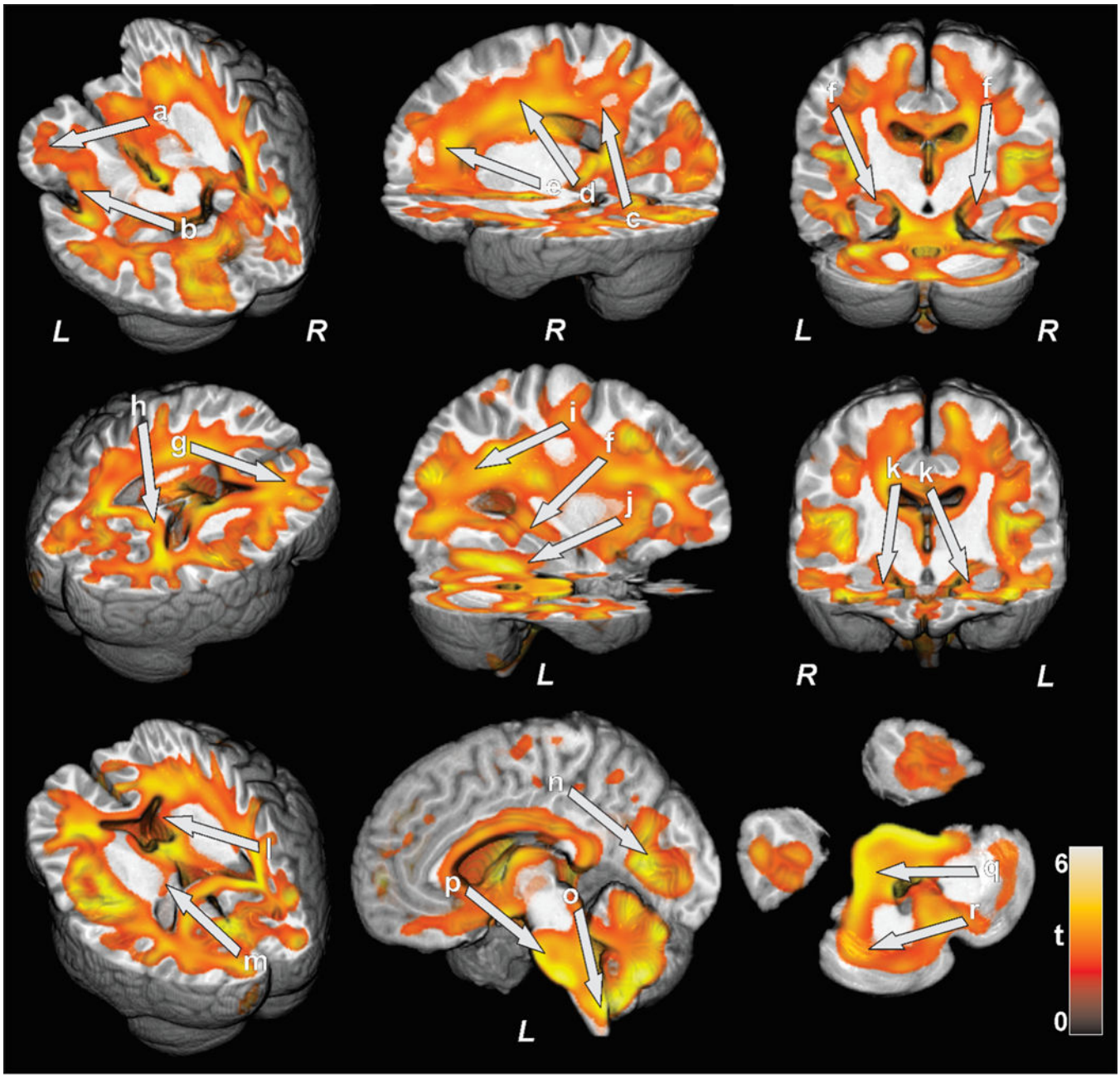

Figure 2:

Brain regions with altered myelin values in HF patients over controls included the bilateral prefrontal cortices (a), insula (b), anterior, mid, posterior cingulate (c,d,e), hippocampus (f), frontal white matter (g), corpus callosum (h), occipital white matter (i), parahippocampal gyrus (j), amygdala (k), caudate (l), thalamus (m), lingual gyrus (n), medulla (o), pons (p), cerebellar peduncle (q) and cortices (r). All images are in neurological convention (L = left; R = right).Color bar indicates t-statistic values.

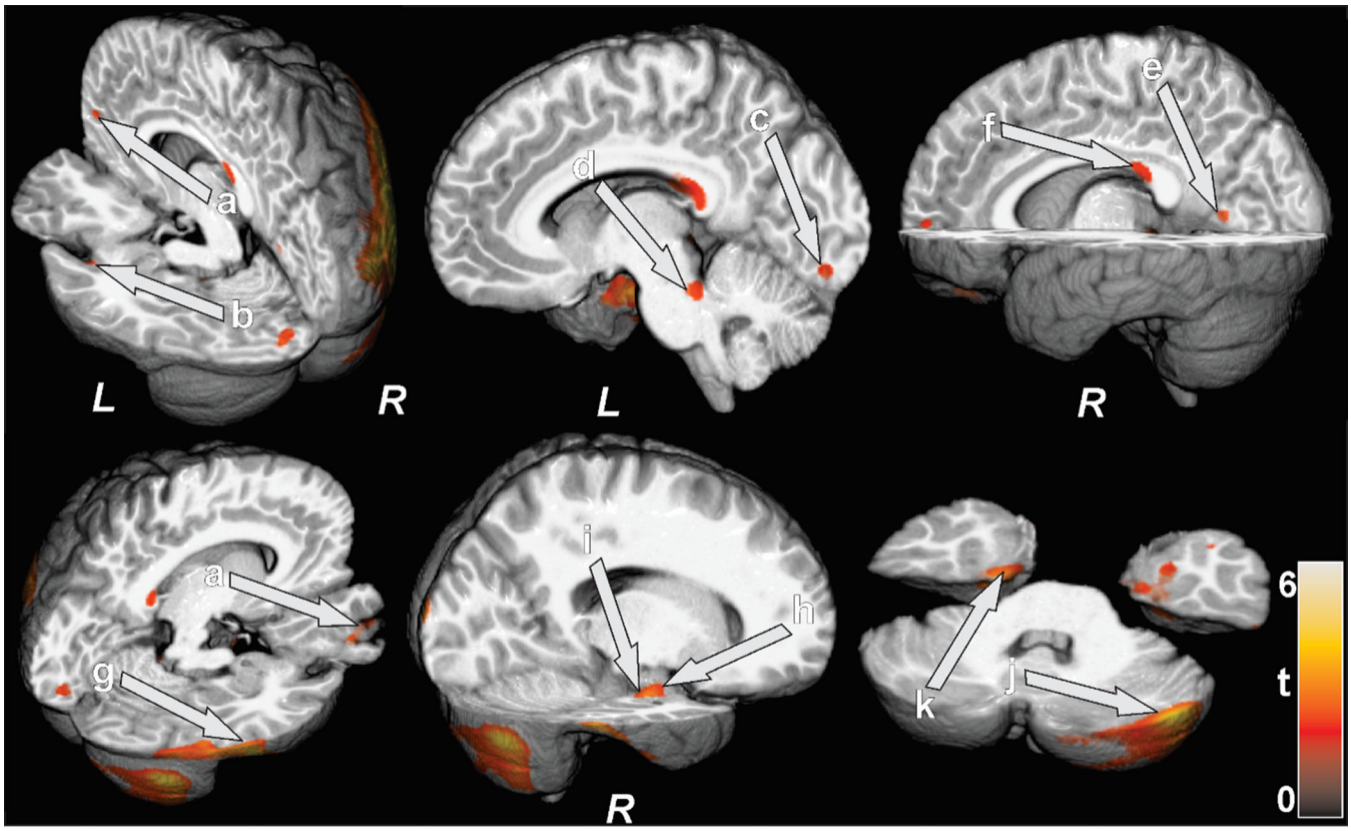

Figure 3:

HF female patient showing widespread myelin changes over male HF patient in prefrontal cortices (a), insula (b), occipital cortices (c), pons (d), lingual gyrus (e), corpus callosum (f), temporal cortices (g), amygdala (h), hippocampus (i), cerebellar cortices (j), and parahippocampal gyrus (k). All images are in neurological convention (L = left; R = right).Color bar indicates t-statistic values.

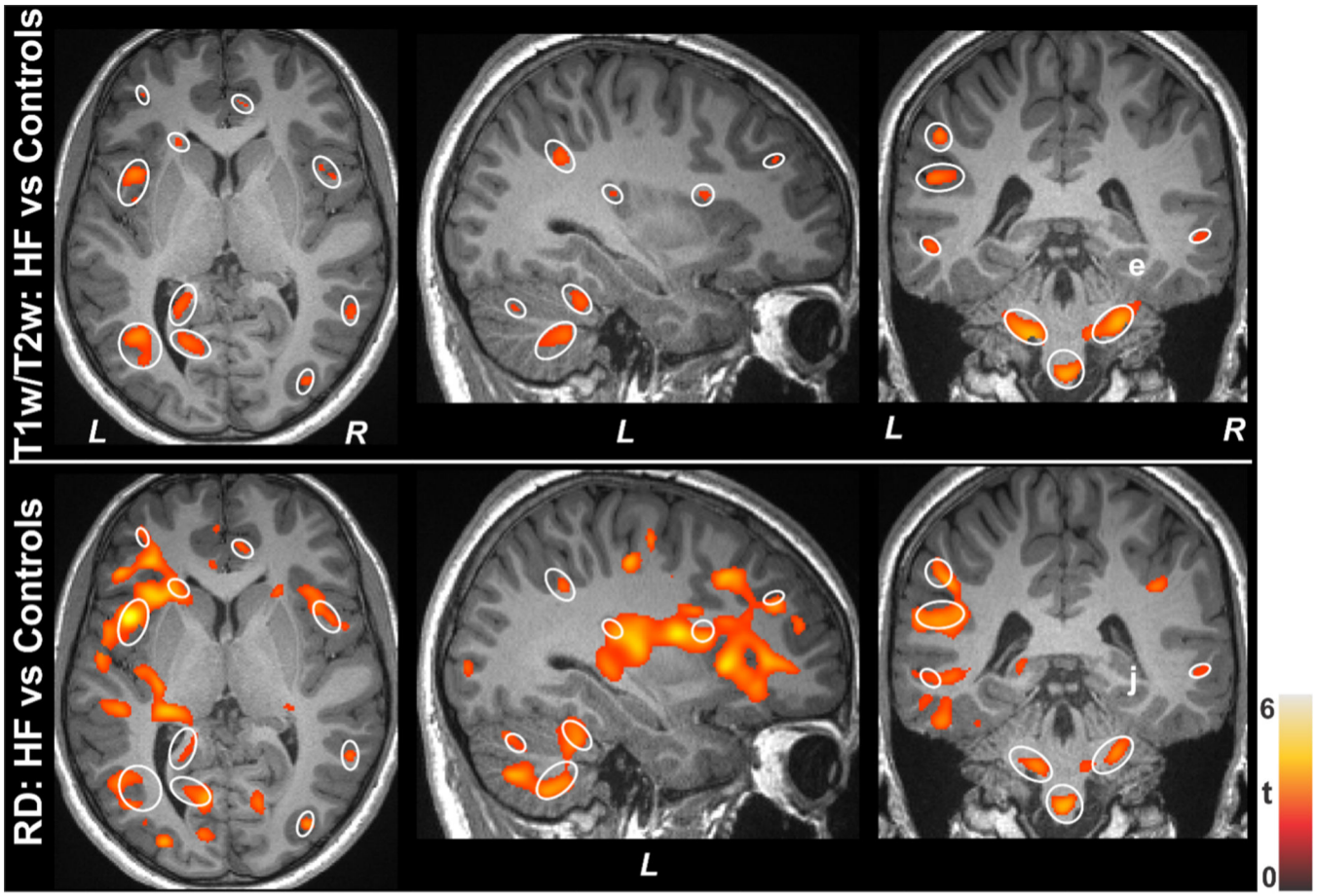

Figure 4:
White marked areas showing brain sites with significant changes in T1-weighted/T2-weighted and RD values in HF patients over control subjects.

Table 1:

Demographics and other variables of heart failure (HF) and control subjects. Values are presented as Mean±SD.

Variables	HF [n=63]	Controls [n=129]	*P* values
Age (years)	54.6±7.9	53.0±6.0	0.142
Sex (Male: Female)	45:18	81:48	0.237
BMI (kg/m^2)	28.5±5.4	25.8±3.7	<0.001
Heart rate (beats/min)	72.8±13.0 [n=46]	71.9±11.3 [n=85]	0.685
Systolic BP (mmHg)	110.2±18.8 [n=46]	120.3±16.7 [n=85]	0.002
Diastolic BP (mmHg)	68.6±11.5 [n=46]	77.7±13.1 [n=85]	<0.001
PSQI	6.8±4.1 [n=53]	3.9±2.5 [n=122]	<0.001
ESS	7.5±4.1 [n=52]	5.2±3.2 [n=122]	<0.001
BDI-II	9.2±7.4 [n=53]	3.3±3.8 [n=122]	<0.001
BAI	9.5±9.3 [n=53]	3.0±3.8 [n=122]	<0.001
Global MoCA	24.7±3.5 [n=46]	26.9±2.2 [n=85]	<0.001
Visuospatial	4.0±1.2 [n=46]	4.5±0.8 [n=85]	0.016
Naming	2.9±0.2 [n=46]	2.9±0.3 [n=85]	0.918
Attention	5.0±1.3 [n=46]	5.4±0.8 [n=85]	0.073
Language	2.2±0.9 [n=46]	2.5±0.8 [n=85]	0.049
Abstraction	1.9±0.4 [n=46]	2.0±0.1 [n=85]	0.142
Delayed recall	2.9±1.6 [n=46]	3.6±1.4 [n=85]	0.007
Orientation	6.0±0.0 [n=46]	6.0±0.2 [n=85]	0.159

HF=Heart failure; SD=Standard deviation; BMI=Body mass index; BP=Blood pressure; PSQI=Pittsburgh Sleep Quality Index; ESS=Epworth Sleepiness Scale; BDI-II=Beck Depression Inventory II; BAI=Beck Anxiety Inventory; MoCA=Montreal Cognitive Assessment.

Table 2:

HF patient variables and sex differences. Values are presented as Mean ± SD or % of patients.

Variables	HF [n=63]		
	Male [n=45]	Female [n=18]	*P* values
Age (years)	54.3±8.0	55.4±8.0	0.629
BMI (kg/m^2)	28.1±4.9	29.5±6.5	0.356
HR (beats/min)	72.7±12.4 [n=33]	73.1±15.1 [n=13]	0.933
SBP (mmHg)	109.3±16.7 [n=33]	112.6±23.9 [n=13]	0.592
DBP (mmHg)	70.5±11.7 [n=33]	63.8±9.8 [n=13]	0.075
PSQI	6.7±4.4 [n=39]	7.1±3.2 [n=14]	0.752
ESS	7.7±4.0 [n=38]	6.9±4.5 [n=14]	0.500
BDI-II	9.1±6.6 [n=39]	9.4±9.4 [n=14]	0.897
BAI	9.0±9.3 [n=39]	10.9±9.6 [n=14]	0.518
MoCA	24.3±3.6 [n=33]	25.8±3.3 [n=13]	0.218
Visuospatial	3.9±1.2 [n=33]	4.2±1.1 [n=13]	0.583
Naming	3.0±0.2 [n=33]	2.8±0.4 [n=13]	0.274
Attention	5.3±1.0 [n=33]	4.3±1.8 [n=13]	0.087
Language	2.0±0.9 [n=33]	2.6±0.7 [n=13]	0.036
Abstraction	1.9±0.5 [n=33]	1.9±0.3 [n=13]	0.759
Delayed Recall	2.5±1.7 [n=33]	3.8±1.0 [n=13]	0.002
Orientation	6.0±0.0 [n=33]	6.0±0.0 [n=13]	1.000
LVEF (%)	27.9±7.9	32.2±10.3	0.079
Systolic dysfunction	44%	85%	
Diastolic dysfunction	9%	0%	
Systolic Diastolic dysfunction	47%	15%	
NYHA Class I	13%	15%	
NYHA Class II	65%	69%	
NYHA Class III	23%	15%	
Ischemic Cardiomyopathy	63%	38%	
Atrial Fibrillation	23%	0%	
Abnormal Sinus Rhythm	15%	11%	
Diuretics	91%	77%	
Beta-blocker	88%	100%	
Angiotensin	19%	46%	
ACE inhibitors	73%	61%	
Hypertension	48%	56%	
Diabetes	27%	44%	

Variables	HF [n=63]		
	Male [n=45]	Female [n=18]	*P* values
Heart attack	27%	15%	

HF=Heart failure; SD=Standard deviation; BMI=Body-mass-index; HR=Heart rate; SBP=Systolic blood pressure; DBP=Diastolic blood pressure; PSQI=Pittsburgh Sleep Quality Index; ESS=Epworth Sleepiness Scale; BDI-II=Beck Depression Inventory II; BAI=Beck Anxiety Inventory; MoCA=Montreal Cognitive Assessment; LVEF = Left ventricular ejection fraction.

Table 3:

Regional brain myelin values from HF and control subjects corrected for age and sex.

	Left hemisphere				Right Hemisphere			
	HF Mean±SD	**Control Mean±SD**	**P- values**	**F**	**HF Mean±SD**	**Control Mean±SD**	**P- values**	**F**
Amygdala	0.37±0.06	0.40±0.06	<0.001	12.5	0.37±0.06	0.40±0.06	<0.001	11.4
Ant Cingulate	0.42±0.07	0.46±0.07	<0.001	12.9	0.39±0.06	0.43±0.06	<0.001	15.1
M Cingulate	0.52±0.09	0.57±0.09	<0.001	13.9	0.51±0.09	0.56±0.09	<0.001	14.6
Post Cingulate	0.54±0.10	0.59±0.10	<0.001	13.7	0.56±0.10	0.62±0.10	<0.001	14.2
Ant Insula	0.35±0.06	0.39±0.05	<0.001	20.6	0.36±0.06	0.40±0.06	<0.001	13.2
Post Insula	0.36±0.06	0.41±0.06	<0.001	20.7	0.39±0.07	0.43±0.07	<0.001	17.1
Basal Forebr	0.27±0.06	0.31±0.06	<0.001	14.2	0.23±0.05	0.26±0.05	<0.001	13.6
Caudate	0.46±0.11	0.52±0.11	<0.001	11.6	0.38±0.10	0.44±0.10	<0.001	13.0
Cerebell Cort	0.49±0.09	0.55±0.09	<0.001	15.7	0.53±0.09	0.58±0.09	<0.001	13.5
Cerebell Verm	0.53±0.08	0.57±0.08	<0.001	12.1	0.55±0.09	0.59±0.09	0.001	11.0
Hippocampus	0.43±0.07	0.47±0.07	<0.001	14.7	0.43±0.07	0.48±0.07	<0.001	15.6
Hypothalamus	0.36±0.08	0.41±0.08	<0.001	13.8	0.27±0.06	0.31±0.06	<0.001	18.7
I Occi GM	0.56±0.10	0.63±0.10	<0.001	17.6	0.54±0.10	0.61±0.10	<0.001	16.4
M Occi GM	0.52±0.10	0.58±0.10	<0.001	19.4	0.50±0.09	0.56±0.09	<0.001	16.6
S Occi GM	0.53±0.10	0.59±0.10	<0.001	15.9	0.53±0.10	0.59±0.10	<0.001	15.7
I Temp GM	0.51±0.09	0.57±0.09	<0.001	15.5	0.50±0.08	0.55±0.08	<0.001	17.2
Lingual Gyrus	0.48±0.08	0.53±0.08	<0.001	17.4	0.48±0.08	0.53±0.08	<0.001	16.7
M Frontal GM	0.46±0.09	0.52±0.09	<0.001	16.9	0.45±0.09	0.51±0.09	<0.001	17.2
M Temp GM	0.50±0.09	0.56±0.09	<0.001	17.6	0.48±0.08	0.53±0.08	<0.001	16.3
S Temp GM	0.51±0.09	0.56±0.09	<0.001	15.1	0.46±0.08	0.51±0.08	<0.001	14.7
Parahippo Gyr	0.43±0.07	0.47±0.07	<0.001	12.2	0.44±0.07	0.48±0.07	<0.001	11.7
Prefrontal Cort	0.45±0.07	0.49±0.07	0.001	10.5	0.36±0.05	0.39±0.05	<0.001	12.5
Putamen	0.59±0.11	0.65±0.11	0.002	10.2	0.50±0.10	0.54±0.10	0.003	9.1
S Parietal GM	0.49±0.10	0.55±0.10	<0.001	15.2	0.47±0.09	0.53±0.09	<0.001	17.9
Thalamus	0.49±0.11	0.55±0.11	<0.001	12.6	0.50±0.10	0.57±0.10	<0.001	14.5
Cerebell Ped	0.62±0.11	0.69±0.11	<0.001	18.9	0.66±0.12	0.73±0.11	<0.001	17.3
Corpus Callos	0.45±0.10	0.50±0.10	<0.001	11.8	0.42±0.10	0.47±0.10	0.002	10.2
External Caps	0.58±0.11	0.63±0.11	0.001	10.6	0.57±0.10	0.62±0.10	0.003	9.3
Frontal WM	0.77±0.13	0.84±0.13	<0.001	13.8	0.75±0.13	0.82±0.13	<0.001	13.2
Medulla	0.45±0.09	0.51±0.09	<0.001	18.1	0.47±0.09	0.52±0.09	<0.001	17.0
Pons	0.69±0.13	0.78±0.13	<0.001	19.2	0.66±0.12	0.75±0.12	<0.001	20.5
I Occi WM	0.59±0.10	0.66±0.10	<0.001	16.5	0.57±0.10	0.63±0.10	<0.001	15.2
M Occi WM	0.55±0.10	0.61±0.10	<0.001	15.6	0.52±0.10	0.58±0.10	<0.001	15.1
S Occi WM	0.57±0.11	0.63±0.11	<0.001	13.6	0.55±0.10	0.62±0.10	<0.001	17.1
I Temp WM	0.70±0.12	0.77±0.12	<0.001	14.6	0.72±0.12	0.78±0.12	<0.001	12.0
M Temp WM	0.53±0.09	0.58±0.09	<0.001	16.1	0.56±0.10	0.62±0.10	<0.001	15.8

	Left hemisphere				Right Hemisphere			
	HF Mean±SD	**Control Mean±SD**	**P- values**	**F**	**HF Mean±SD**	**Control Mean±SD**	**P- values**	**F**
S Temp WM	0.53±0.10	0.59±0.10	<0.001	14.1	0.58±0.10	0.64±0.10	<0.001	14.3
S Parietal WM	0.48±0.10	0.54±0.10	<0.001	16.3	0.48±0.10	0.55±0.10	<0.001	18.6

HF = Heart failure; SD = Standard deviation; Ant = Anterior; M = Middle; Post = Posterior; Forebr = Forebrain; Cerebell = Cerebellar; Cort = Cortex; Verm = Vermis; I = Inferior; Occi = Occipital; GM = Gray Matter; S = Superior; Temp = Temporal; Parahippo = Parahippocampal; Gyr = Gyrus; Ped = Peduncle; Callos = Callosum; Caps = Capsule; WM = White Matter.

Table 4:

Regional brain myelin values from male and female heart failure (HF) patients corrected for age.

	Male HF [n=45] (Mean±SD)	Female HF [n=18] (Mean±SD)	*F*	*P* values
R Ven Med Prefrontal Cortex	0.40±0.08	0.34±0.08	7.4	0.009
R Frontal Cortex	0.37±0.09	0.30±0.09	8.1	0.006
R Hippocampus	0.38±0.06	0.33±0.06	10.3	0.002
R Amygdala	0.34±0.06	0.29±0.06	9.0	0.004
R Parietal Cortex	0.47±0.09	0.40±0.09	8.4	0.005
R Posterior Cingulate	0.45±0.10	0.37±0.10	8.2	0.006
L Pons	0.48±0.09	0.41±0.09	7.8	0.007
L Cerebellar Peduncle	0.44±0.08	0.38±0.08	7.5	0.008
L Insula	0.37±0.07	0.32±0.07	7.2	0.009
L Posterior Corpus Callosum	0.59±0.14	0.47±0.14	8.6	0.005
R Posterior Corpus Callosum	0.56±0.14	0.45±0.14	8.2	0.006
L Colliculus	0.29±0.06	0.25±0.06	7.3	0.009
R Colliculus	0.29±0.06	0.25±0.06	7.2	0.009
L Lingual Gyrus	0.57±0.12	0.47±0.12	8.1	0.006
R Lingual Gyrus	0.57±0.14	0.46±0.14	7.2	0.010
L Cerebellar Cortex	0.45±0.10	0.37±0.10	7.5	0.008
R Cerebellar Cortex	0.51±0.11	0.40±0.11	11.8	0.001
L Parahippocampal Gyrus	0.41±0.06	0.35±0.06	10.8	0.002
R Parahippocampal Gyrus	0.44±0.07	0.37±0.07	10.7	0.002
L Prefrontal Cortex	0.68±0.10	0.60±0.10	8.2	0.006
R Prefrontal Cortex	0.43±0.06	0.37±0.06	10.6	0.002
L Temporal Cortex	0.51±0.10	0.43±0.10	7.1	0.010
R Temporal Cortex	0.59±0.08	0.48±0.08	20.2	<0.001
L Occipital Cortex	0.59±0.14	0.47±0.14	9.1	0.004
R Occipital Cortex	0.67±0.11	0.57±0.11	12.1	<0.001
L Temporal White Matter	0.52±0.09	0.45±0.09	7.7	0.007

SD = Standard deviation; R = Right; Ven = Ventral; Med = Medial; L = Left.

Table 5:

The magnitude of t-scores obtained from T1-w/T2-w and RD maps from various ROIs in HF and controls.

	Left hemisphere (t score)		Right Hemisphere (t score)	
	HF (T1/T2, RD)	Control (T1/T2, RD)	HF (T1/T2, RD)	Control (T1/T2, RD)
Cingulate	7.4, 7.1	21.4, 12.8	8.3, 7.8	16.7, 10.7
Insula	29.3, 10.6	39.7, 14.1	16.5, 9.9	29.3, 15.5
Caudate	2.9, 7.7	4.6, 10.3	7.6, 7.0	14.1, 10.4
Cerebellar WM	14.0, 20.1	30.6, 31.9	23.8, 18.0	32.8, 32.2
Cerebral WM	22.5, 21.9	32.8, 38.3	22.8, 19.8	33.2, 32.0
Occi Gyrus	10.3, 11.4	13.4, 16.8	3.3, 10.0	3.8, 12.7
Lingual Gyrus	9.9, 18.0	11.2, 18.9	1.1, 15.7	1.6, 22.0
Frontal Gyrus	24.5, 14.2	32.0, 22.8	25.8, 15.9	42.9, 22.3
Temp Gyrus	4.7, 2.0	5.3, 7.0	7.1, 2.3	10.1, 3.0
Parahippo Gyrus	24.1, 9.3	38.2, 19.0	17.0, 9.7	31.4, 18.4
Prefrontal Cortex	17.7, 11.6	28.2, 11.2	24.8, 14.2	40.2, 13.0
Putamen	12.1, 16.7	23.9, 37.2	14.5, 15.2	27.8, 32.1
Parietal Gyrus	17.3, 10.3	30.3, 22.8	17.9, 12.4	28.3, 22.2
Thalamus	7.7, 0.7	9.5, 2.3	4.1, 0.3	5.9, 1.1

HF = Heart failure; WM = White Matter; Occi = Occipital; Temp = Temporal; Parahippo = Parahippocampal.